CHAPTER IV
RESULTS AND DISCUSSION

4.1 Effect of Feed Composition on *m*- and *p*-CNB Crystallization

Different concentrations of *m*-CNB (20.0, 30.0, 50.0, 61.0, 62.0, 62.5, 62.9, 63.5, 64.0, 65.0, 67.5, 70.0, 80.0, and 90 wt%) were used to study the *m*- and *p*-CNB crystallization and construct the binary phase diagram. Seven grams of solid *m*- and *p*-CNB were melted to obtain a homogeneous liquid solution. The liquid mixture was measured for the CNB compositions using the GC. Then, the liquid mixture in the crystallizer was cooled by the cooling water to a crystallization temperature. All solids were collected from the crystallizer, washed, and dissolved with hexane. The dissolved solids were measured for the CNB compositions by the GC. Table 4.1 shows the crystallization temperature and the feed and solid compositions from two to three separate experiments. It can be clearly seen that the experiment is reproducible.

The crystallization of the feed below the eutectic composition (20, 30, 50, 61, 62, and 62.5 wt% *m*-CNB) results in the solid form. The composition is rich in *p*-CNB. On the contrary, when the feed composition at the eutectic composition (62.9 wt% *m*-CNB) is cooled down to the crystallization temperature at 22.5 °C, an amorphous solid with the composition close to the feed composition can be observed. Crystallization of the feed above the eutectic composition results in the solid form, which is the same with that below the eutectic composition but the composition is rich in *m*-CNB. Figure 4.1 compares the data obtained from this work and that of Sulzer Chemtech Pte., Ltd. It can be seen that the results are relatively close. On a whole, the result shows the purity of the solid composition is not close to 100 wt%. In the industrial crystallization practice, many bulk-produced chemicals with purity more than 95 percent are often accepted as justifying the designation "pure". Generally, crystals contain foreign impurities or called "inclusion" (Mullin, 2001).

Table 4.1 Composition of *m*- and *p*-CNB in the feeds and solids after crystallization

Feed	Feed composition (wt%)		Solid composition (wt%)		Crystallization temperature (°C)
	m-CNB	*p*-CNB	*m*-CNB	*p*-CNB	
Below the eutectic	20.15 [1]	79.95 [1]	3.74 [1]	96.26 [1]	67.0
	20.17 [2]	79.93 [2]	3.57 [2]	96.43 [2]	67.5
	30.11 [1]	69.89 [1]	2.18 [1]	97.82 [1]	57.0
	30.09 [2]	69.91 [2]	4.65 [2]	95.35 [2]	57.0
	50.17 [1]	49.83 [1]	4.89 [1]	95.11 [1]	38.0
	50.06 [2]	49.94 [2]	4.98 [2]	95.02 [2]	38.0
	61.09 [1]	38.91 [1]	2.63 [1]	97.37 [1]	24.0
	61.04 [2]	38.96 [2]	4.71 [2]	95.29 [2]	23.5
	61.08 [3]	38.92 [3]	4.72 [3]	95.28 [3]	24.0
	62.18 [1]	37.82 [1]	2.75 [1]	97.27 [1]	23.5
	62.06 [2]	37.94 [2]	5.34 [2]	94.66 [2]	23.5
	62.02 [3]	37.98 [3]	5.49 [3]	94.51 [3]	23.5
	62.57 [1]	37.43 [1]	2.52 [1]	97.48 [1]	22.5
	62.52 [2]	37.48 [2]	3.48 [2]	96.52 [2]	23.0
	62.51 [3]	37.49 [3]	3.11 [3]	96.89 [3]	23.0
The eutectic	62.91 [1]	37.09 [1]	62.95 [1]	37.05 [1]	22.5
	62.92 [2]	37.08 [2]	62.90 [2]	37.10 [2]	22.5
	62.95 [3]	37.05 [3]	62.93 [3]	37.07 [3]	22.5
Above the eutectic	63.52 [1]	36.48 [1]	93.66 [1]	7.34 [1]	23.5
	63.65 [2]	36.35 [2]	96.17 [2]	3.82 [2]	24.0
	63.59 [3]	36.41 [3]	96.83 [3]	3.17 [3]	23.5
	64.18 [1]	35.82 [1]	98.26 [1]	1.74 [1]	23.5
	64.08 [2]	35.92 [2]	98.17 [2]	1.83 [2]	23.5
	64.13 [3]	35.87 [3]	98.42 [3]	1.58 [3]	23.5

Table 4.1(cont.) Composition of *m*- and *p*-CNB in the feed and solid after crystallization

Feed	Feed composition (wt%)		Solid composition (wt%)		Crystallization temperature (°C)
	m-CNB	*p*-CNB	*m*-CNB	*p*-CNB	
Above the eutectic	65.04 [1]	34.96 [1]	95.79 [1]	4.21 [1]	23.5
	65.08 [2]	34.92 [2]	98.17 [2]	1.83 [2]	23.5
	65.11 [3]	34.89 [3]	95.13 [3]	4.87 [3]	24.0
	67.59 [1]	32.41 [1]	95.69 [1]	4.31 [1]	24.5
	67.55 [2]	32.45 [2]	96.34 [2]	3.66 [2]	24.5
	67.51 [3]	32.49 [3]	96.51 [3]	3.49 [3]	24.5
	70.27 [1]	29.73 [1]	97.70 [1]	2.30 [1]	26.0
	70.13 [2]	29.07 [2]	98.33 [2]	1.67 [2]	26.0
	70.09 [3]	29.91 [3]	98.79 [3]	1.21 [3]	26.0
	80.17 [1]	19.83 [1]	97.70 [1]	2.30 [1]	28.5
	80.02 [2]	19.98 [2]	97.63 [2]	2.37 [2]	27.5
	90.16 [1]	9.84 [1]	98.08 [1]	1.92 [1]	34.0
	90.08 [2]	9.92 [2]	97.89 [2]	2.11 [2]	34.0

* The number in the parenthesis refers to number of run.
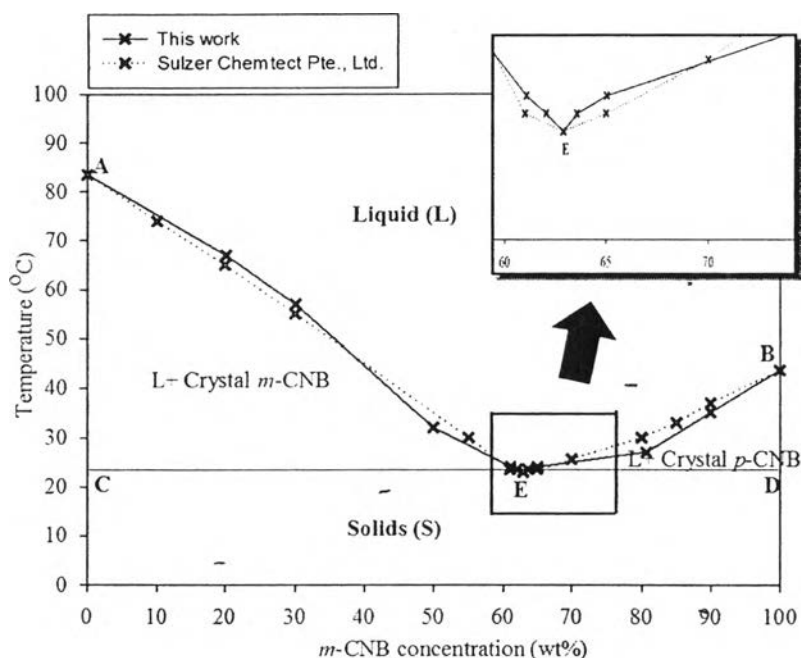
Figure 4.1 Composition of the binary phase diagram of *m*- and *p*-CNB between this work and that from Sulzer Chemtech Pte., Ltd.

4.2 Effects of Zeolites and Amorphous Materials on the Crystallization and Composition of *m*- and *p*-CNB

4.2.1 Effects of Zeolites on the CNB Solid Composition and Crystallization Temperature

The effects of KY zeolite on the CNB crystal composition and crystallization temperature were investigated. Five grains of the KY zeolite were added at the center of the CNB mixture in the crystallizer. The feed composition, solid composition, and crystallization temperature are shown in Table 4.2. With the presence of the KY zeolite, the crystallization of the feed with the composition between 20.0 – 64.0 wt% *m*-CNB and 67.5 – 90.0 wt% *m*-CNB results in the crystal form. The crystals obtained from the crystallization of the feed between 20.0 – 64.0 wt% *m*-CNB are rich in *p*-CNB, while those from 67.5 – 90.0 wt% *m*-CNB are rich in *m*-CNB. The eutectic composition of the system with the KY zeolite is now at 65.5 wt% *m*-CNB with 18.5 °C eutectic temperature.

Figure 4.2 compares the solid liquid phase diagram of *m*- and *p*-CNB without and with the KY zeolite. From the feed at 62.9 wt% *m*-CNB, which is the eutectic composition of the *m*- and *p*-CNB mixture, the crystallization with the addition of KY zeolite clearly results in the crystal formation, not the amorphous solid as in the case, where this is no zeolite. The eutectic composition is 65.5 wt% *m*-CNB, which is about 3 wt% *m*-CNB higher in the *m*-CNB composition than the amorphous solid composition, 62.9 wt% *m*-CNB, from the system without the zeolite. In addition, the new eutectic temperature is about 4 °C lower, 18.5 °C compared to 22.9 °C.

Table 4.2 Composition of *m*- and *p*-CNB in the solids after crystallization with the KY zeolite

Feed	Feed composition (wt%)		Solid composition (wt%)		Crystallization temperature (°C)
	m-CNB	*p*-CNB	*m*-CNB	*p*-CNB	
Below the eutectic	20.08 [1]	79.92 [1]	2.82 [1]	97.18 [1]	67.5
	20.15 [2]	79.85 [2]	3.87 [2]	96.13 [2]	67.5
	30.21 [1]	69.89 [1]	1.26 [1]	98.74 [1]	58.0
	30.05 [2]	69.95 [2]	3.44 [2]	96.56 [2]	58.0
	49.98 [1]	50.02 [1]	2.41 [1]	97.59 [1]	38.0
	50.02 [2]	49.98 [2]	1.46 [2]	98.54 [2]	38.0
	61.09 [1]	39.91 [1]	2.26 [1]	97.74 [1]	24.0
	61.02 [2]	38.98 [2]	3.87 [2]	96.13 [2]	24.0
	61.01 [3]	38.99 [3]	2.33 [3]	97.67 [3]	24.0
	62.02 [1]	37.98 [1]	1.73 [1]	98.27 [1]	23.5
	62.12 [2]	37.88 [2]	2.49 [2]	97.51 [2]	24.0
	62.06 [3]	37.94 [3]	3.29 [3]	96.71 [3]	24.0
	62.52 [1]	37.48 [1]	1.65 [1]	98.35 [1]	22.0
	62.54 [2]	37.46 [2]	2.18 [2]	97.92 [2]	22.0
	62.58 [3]	37.42 [3]	2.74 [3]	97.26 [3]	22.0

Table 4.2 (cont.) Composition of *m*- and *p*-CNB in the solids after crystallization with the KY zeolite

Feed	Feed composition (wt%)		Solid composition (wt%)		Crystallization temperature (°C)
	m-CNB	*p*-CNB	*m*-CNB	*p*-CNB	
Below the eutectic	62.93 [1]	37.07 [1]	1.05 [1]	98.95 [1]	20.5
	62.94 [2]	37.06 [2]	3.05 [2]	96.05 [2]	20.5
	62.91 [3]	37.09 [3]	3.25 [3]	96.75 [3]	20.0
	63.45 [1]	36.55 [1]	1.48 [1]	98.52 [1]	20.0
	63.53 [2]	36.47 [2]	3.61 [2]	96.39 [2]	19.5
	63.56 [3]	36.44 [3]	2.81 [3]	97.19 [3] -	19.5
	64.09 [1]	35.91 [1]	2.58 [1]	97.42 [1]	19.5
	64.15 [2]	35.85 [2]	2.62 [2]	97.38 [2]	19.5
	64.07 [3]	35.93 [3]	2.64 [3]	97.36 [3]	19.5
The eutectic	65.56 [1]	34.44 [1]	65.64 [1]	34.36 [1]	18.5
	65.61 [2]	34.39 [2]	65.69 [2]	34.31 [2]	18.5
	65.57 [3]	34.43 [3]	65.43 [3]	34.36 [2]	18.5
Above the eutectic	67.55 [1]	32.45 [1]	96.21 [1]	3.79 [1]	20.0
	67.48 [2]	32.52 [2]	97.83 [2]	2.17 [2]	20.5
	67.52 [3]	32.48 [3]	97.75 [3]	2.25 [2]	20.0
	70.05 [1] -	29.95 [1]	95.53 [1]	4.47 [1]	20.5
	70.25 [2] _	29.75 [2]	97.15 [2]	2.85 [2]	20.5
	70.09 [3]	29.91 [3]	98.12 [3]	1.88 [3]	20.5
	79.93 [1]	20.07 [1]	98.80 [1]	1.20 [1]	27.5
	79.90 [2]	20.10 [2]	97.06 [2]	2.94 [2]	27.5
	90.28 [1]	9.72 [1]	97.84 [1]	2.16 [1]	34.0
	90.16 [2]	9.84 [2]	97.13 [2]	2.87 [2]	34.0

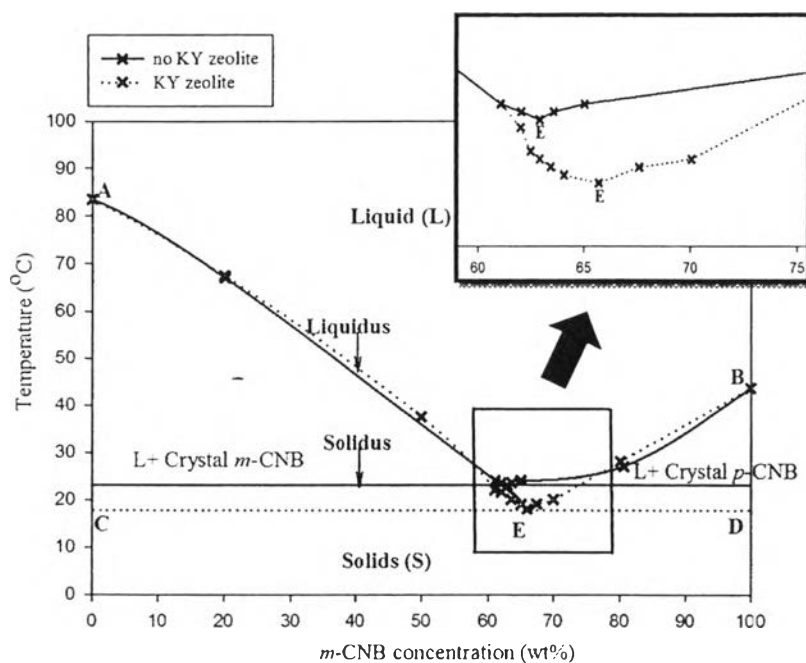* The number in the parenthesis refers to number of run.

Figure 4.2 Liquid solid phase diagram of *m*- and *p*-CNB without and with the KY zeolite.

Table 4.3 shows the feed composition, solid composition, and crystallization temperature of *m*- and *p*-CNB with the presence of the BaX zeolite. The crystallization of the feed with 20.0 – 65.0 wt% *m*-CNB results in the crystals rich in *p*-CNB. On the contrary, when the feed 67.5 – 80.0 wt% *m*-CNB is crystallized, the crystals are rich in *m*-CNB. Like the system with the KY zeolite, the presence of the BaX zeolite affects the eutectic composition and temperature of *m*- and *p*-CNB. The eutectic composition and temperature are about 66.0 wt% *m*-CNB and 18.0 °C. Comparison of the solid liquid phase diagram of *m*- and *p*-CNB without and with the BaX zeolite is shown in Figure 4.4. It was found that the eutectic composition is at 66.0 wt% *m*-CNB and the eutectic temperature is about 4 °C lower than that without the zeolite.

Table 4.3 Composition of *m*- and *p*-CNB in the solids after crystallization with the BaX zeolite

Feed	Feed composition (wt%)		Solid composition (wt%)		Crystallization temperature (°C)
	m-CNB	*p*-CNB	*m*-CNB	*p*-CNB	
Below the eutectic	20.05 [1]	79.95 [1]	1.21 [1]	98.89 [1]	67.5
	20.12 [2]	79.88 [2]	1.89 [2]	98.11 [2]	67.0
	49.98 [1]	69.02 [1]	1.28 [1]	98.72 [1]	38.5
	50.01 [2]	69.99 [2]	2.41 [2]	97.59 [2]	38.5
	61.99 [1]	38.01 [1]	1.94 [1]	98.06 [1]	21.5
	62.06 [2]	37.94 [2]	2.64 [2]	97.35 [2]	21.0
	62.02 [3]	37.98 [3]	1.89 [3]	98.11 [3]	21.0
	63.51 [1]	36.49 [1]	1.18 [1]	98.82 [1]	19.5
	63.57 [2]	36.43 [2]	1.50 [2]	98.50 [2]	19.5
	65.05 [1]	34.95 [1]	2.35 [1]	97.65 [1]	18.5
	64.97 [2]	34.03 [2]	1.78 [2]	98.22 [2]	19.0
	65.05 [3]	34.95 [3]	2.49 [3]	97.51 [3]	18.5
	65.05 [1]	34.95 [1]	2.35 [1]	97.65 [1]	18.5
	64.97 [2]	34.03 [2]	1.78 [2]	98.22 [2]	19.0
	65.05 [3]	34.95 [3]	2.49 [3]	97.51 [3]	18.5
The eutectic	65.99 [1]	34.01 [1]	66.02 [1]	33.98 [1]	18.0
	66.02 [2]	33.98 [2]	66.05 [2]	33.95 [2]	18.0
	66.05 [3]	33.95 [3]	66.03 [3]	33.97 [3]	18.0
Above the eutectic	67.56 [1]	32.44 [1]	97.65 [1]	2.35 [1]	19.0
	67.47 [2]	32.53 [2]	97.97 [2]	2.03 [2]	19.5
	67.51 [3]	32.49 [3]	97.21 [3]	2.79 [3]	19.5
	69.97 [1]	29.03 [1]	98.43 [1]	1.57 [1]	20.0
	70.04 [2]	29.96 [2]	97.13 [2]	1.87 [2]	20.0
	80.11 [1]	20.89 [1]	98.54 [1]	1.46 [1]	28.0
	80.06 [2]	20.94 [2]	98.70 [2]	1.30 [2]	27.5

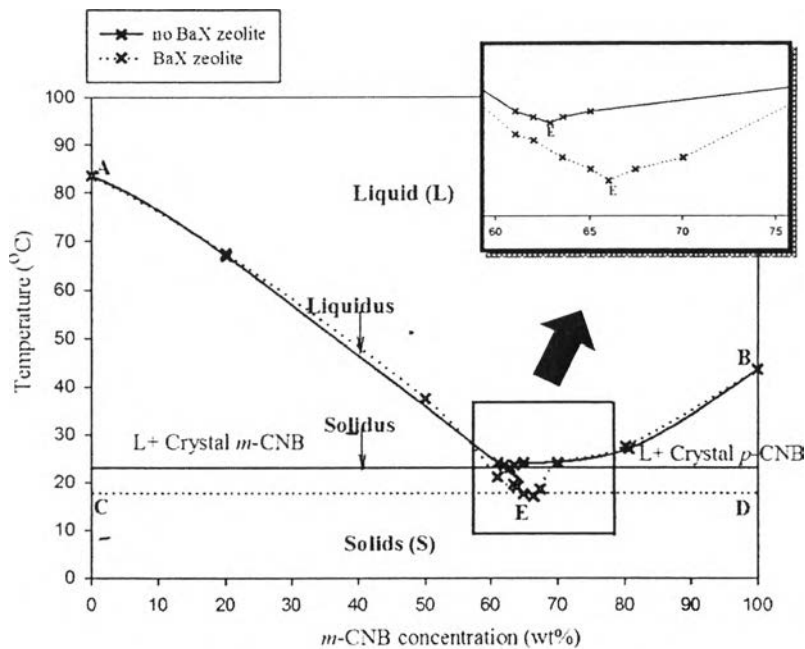* The number in the parenthesis refers to number of run.

Figure 4.3 Liquid solid phase diagram of *m*- and *p*-CNB without and with the BaX zeolite.

NaX zeolite is then chosen for the study as the zeolite has high *m*-CNB selectivity than the KY and BaX zeolites (Leardsakulthong, 2008). Table 4.4 shows the feed composition, solid composition, and crystallization temperature of *m*- and *p*-CNB in the presence of NaX zeolite. Crystallization of the feed with 20.0 – 65.0 wt% *m*-CNB results in the crystals rich in *p*-CNB, while crystallization of the feed with 67.5 – 90.0 wt% *m*-CNB results in the crystals rich in *m*-CNB. The eutectic composition of the system with the NaX zeolite is now at 66.5wt% *m*-CNB with 17.0 °C eutectic temperature. Comparison of the solid liquid phase diagrams of *m*- and *p*-CNB without and with NaX zeolite is shown in Figure 4.5. The eutectic composition from the system with the zeolite is about 3.5 wt% *m*-CNB higher than that the without the zeolite, while the crystallization temperature is about 5.5 °C lower than that without the zeolite. It can be seen that the presence of the NaX zeolite results in about the same affects as the KY and BaX zeolites despite its high *m*-CNB selectivity.

Comparison among the effects of the KY, BaX, and NaX zeolites on the crystallization of *m*- and *p*-CNB shows that the crystallization temperature and eutectic composition of *m*- and *p*-CNB mixture with the presence of the zeolites have

the same trend. That is their presence results in lower crystallization temperature and higher m-CNB in the eutectic composition than the system without the zeolites. Other than that, there is no significant difference between the system with and without the zeolites.

Table 4.4 Composition of m- and p-CNB in the solids after crystallization with the NaX zeolite

Feed	Feed composition (wt%)		Solid composition (wt%)		Crystallization temperature (°C)
	m-CNB	p-CNB	m-CNB	p-CNB	
-	20.09 [1]	79.91[1]	4.29 [1]	95.71 [1]	66.5
	20.04 [2]	79.96[2]	3.58 [2]	96.42 [2]	67.0
	30.09 [1]	69.91[1]	3.59 [1]	96.41 [1]	58.0
	30.07 [2]	69.93[2]	4.71 [2]	95.29 [2]	57.5
	50.03 [1]	49.97 [1]	4.39 [1]	95.61 [1]	37.5
	49.98 [2]	50.02 [2]	6.59 [2]	93.41 [2]	38.0
	61.02 [1]	38.98 [1]	5.33 [1]	94.67 [1]	20.5
	61.09 [2]	38.91 [2]	4.29 [2]	95.71 [2]	21.0
Below the eutectic	61.04 [3]	38.96 [3]	4.45 [3]	95.46 [3]	20.5
	63.52 [1]	36.48 [1]	3.86 [1]	96.14 [1]	19.5
	63.56 [2]	36.44 [2]	5.39 [2]	94.61 [2]	19.5
	63.49 [3]	36.51 [3]	4.49 [3]	95.51 [3]	19.0
	64.10 [1]	35.90 [1]	4.95 [1]	95.05 [1]	19.0
	64.08 [2]	35.92 [2]	3.58 [2]	96.42 [2]	18.5
	63.98 [3]	36.02 [3]	5.14 [3]	94.86 [3]	19.0
	65.11 [1]	34.89 [1]	5.52 [1]	94.48 [1]	17.5
	65.02 [2]	34.98 [2]	4.48 [2]	95.16 [2]	18.0
	65.06 [3]	34.94 [3]	4.18 [3]	95.82 [2]	18.0

Table 4.4 (Cont.) Composition of *m*- and *p*-CNB in the solids after crystallization with the NaX zeolite

Feed	Feed composition (wt%)		Solid composition (wt%)		Crystallization temperature (°C)
	m-CNB	*p*-CNB	*m*-CNB	*p*-CNB	
The eutectic	66.51 [1]	33.49 [1]	66.54 [1]	33.46 [1]	17.0
	66.53 [2]	33.47 [2]	66.48 [2]	33.52 [2]	17.0
	66.49 [3]	33.51 [3]	66.52 [3]	33.48 [3]	17.0
Above the eutectic	67.51 [1]	32.49 [1]	96.17 [1]	3.83 [1]	18.5
	67.56 [2]	32.44 [2]	95.58 [2]	4.42 [2]	18.0
	67.54 [3]	32.48 [3]	95.69 [3]	4.31 [2]	18.5
	70.09 [1]	29.91 [1]	94.14 [1]	5.86 [1]	24.0
	70.11 [2]	29.99 [2]	95.02 [2]	4.98 [2]	24.5
	80.09 [1]	19.91 [1]	96.48 [1]	3.52 [1]	27.5
	80.06 [2]	19.94 [2]	96.78 [2]	3.22 [2]	28.0
	90.12 [1]	9.88 [1]	98.62 [1]	1.38 [1]	34.0
	90.03 [2]	9.97 [2]	97.66 [2]	2.34 [2]	34.0

* The number in the parenthesis refers to number of run.
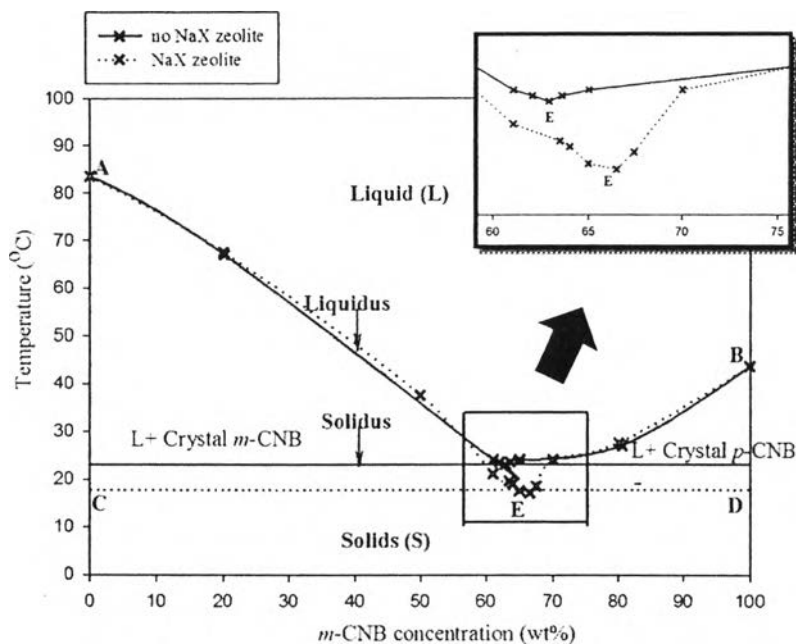
Figure 4.4 Liquid solid phase diagram of *m*- and *p*-CNB without and with the NaX zeolite.

4.2.2 Effects of Amorphous Materials on the CNB Solid Composition and Crystallization Temperature

To further prove the effects of solid materials on the crystallization of *m*- and *p*-CNB, amorphous materials, instead of zeolites, were used. Activated carbon and silica gel were selected, in part, because of their low *m*-CNB selectivity (Leardsakulthong, 2008).

Table 4.5 shows the feed composition, solid composition, and crystallization temperature of *m*- and *p*-CNB system in the presence of the activated carbon. After adding the activated carbon, the crystallization of the feed with 30.0 - 65.0 wt% *m*-CNB results in the crystals rich in *p*-CNB. The eutectic composition is at 66.5 wt% *m*-CNB, which is higher than that of the system without the activated carbon but relatively, the same with the systems with the zeolites. The eutectic temperature is 16.5 °C, which is lower than the one without the activated carbon. The activated carbon has about the same effect on the eutectic temperature as the zeolites Crystallization of the feed with 67.0 – 80.0 wt% *m*-CNB results in the crystals rich in *m*-CNB. Figure 4.5 compares the binary phase diagrams of *m*- and *p*-CNB mixtures without and with the activated carbon. The figure further confirms the effects of the

activated carbon on the phase diagram. That is the crystallization temperature decreases and the eutectic composition increases. Between 30.0 – 65.0 wt% m-CNB and 67.0 – 80.0 wt% m-CNB, the activated carbon hardly affects the phase behavior. It is also clear that the activated carbon and the zeolites have the similar effects on the crystallization of m- and p-CNB mixtures.

Table 4.5 Composition of m- and p-CNB in the solids after crystallization with activated carbon

Feed	Feed composition (wt%)		Solid composition (wt%)		Crystallization temperature (°C)
	m-CNB	p-CNB	m-CNB	p-CNB	
Below the eutectic	30.11 [1]	69.89 [1]	2.72 [1]	97.28 [1]	59.0
	30.04 [2]	69.96 [2]	3.12 [2]	96.88 [2]	58.5
	65.12 [1]	34.88 [1]	7.39 [1]	92.61 [1]	17.5
	65.08 [2]	34.92 [2]	4.36 [2]	95.64 [2]	17.5
	65.03 [3]	34.97 [3]	3.94 [3]	96.06 [3]	18.0
At eutectic	66.52 [1]	34.48 [1]	66.48 [1]	33.52 [1]	17.0
	66.53 [2]	34.47 [2]	66.57 [2]	33.43 [2]	16.5
	66.59 [3]	34.41 [3]	66.50 [3]	33.50 [3]	16.5
Above the eutectic	67.04 [1]	34.96 [1]	95.11 [1]	4.89 [1]	18.0
	67.10 [2]	34.90 [2]	97.04 [2]	2.96 [2]	17.5
	67.07 [3]	34.97 [3]	96.44 [3]	3.56 [3]	18.0
	80.06 [1]	19.94 [1]	97.07 [1]	2.93 [1]	27.5
	80.11 [2]	19.89 [2]	98.83 [2]	1.17 [2]	27.5

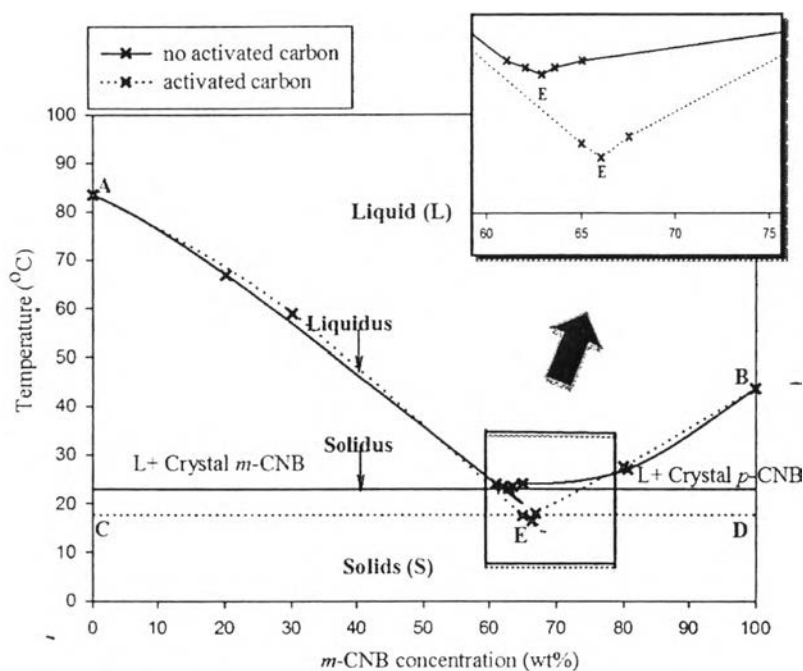* The number in the parenthesis refers to number of run.

Figure 4.5 Liquid solid phase diagram of *m*- and *p*-CNB without and with the activated carbon.

Results of adding silica gel in the crystallization of *m*- and *p*-CNB are shown in Table 4.6. Adding the silica gel into the feed mixture with 30.0 – 65.0 wt% *m*-CNB results in the crystals rich in *p*-CNB. The eutectic composition of the system is at 66.0 wt% *m*-CNB, and the eutectic temperature is 17.0 °C. Comparison between the solid liquid phase diagrams of *m*- and *p*-CNB without and with the silica gel is shown in Figure 4.6. It can be seen that the eutectic composition increases from the system without silica gel, and the eutectic temperature is about 5.0 °C lower than that without the silica gel. The presence of silica gel results in about the same affects as the KY, BaX, and NaX zeolites despite its low *m*-CNB selectivity.

Table 4.6 Composition of *m*- and *p*-CNB in the solids after crystallization with the silica gel

Feed	Feed composition (wt%)		Solid composition (wt%)		Crystallization temperature (°C)
	m-CNB	*p*-CNB	*m*-CNB	*p*-CNB	
Below the eutectic	30.02 [1]	69.98 [1]	3.95 [1]	96.41 [1]	60.0
	30.05 [2]	69.95 [2]	2.74 [2]	97.26 [2]	59.5
	65.07 [1]	34.93 [1]	3.59 [1]	96.41 [1]	18.0
	65.11 [2]	34.89 [2]	1.98 [2]	98.02 [2]	18.5
	65.08 [3]	34.92 [3]	2.29 [3]	97.71 [3]	18.5
At eutectic	66.02 [1]	33.98 [1]	66.05 [1]	33.95 [1]	17.0
	66.09 [2]	33.91 [2]	66.12 [2]	33.88 [2]	17.5
	66.05 [3]	33.95 [2]	66.04 [2]	33.96 [2]	17.0
Above the eutectic	67.54 [1]	32.46 [1]	95.71 [1]	4.29 [1]	18.5
	67.52 [2]	32.48 [2]	98.85 [2]	1.15 [2]	18.5
	67.56 [3]	32.44 [3]	96.23 [3]	3.77 [3]	18.5
	80.09 [1]	9.91 [1]	98.11 [1]	1.89 [1]	27.5
	80.10 [2]	9.90 [2]	98.71 [2]	1.29 [2]	28.0

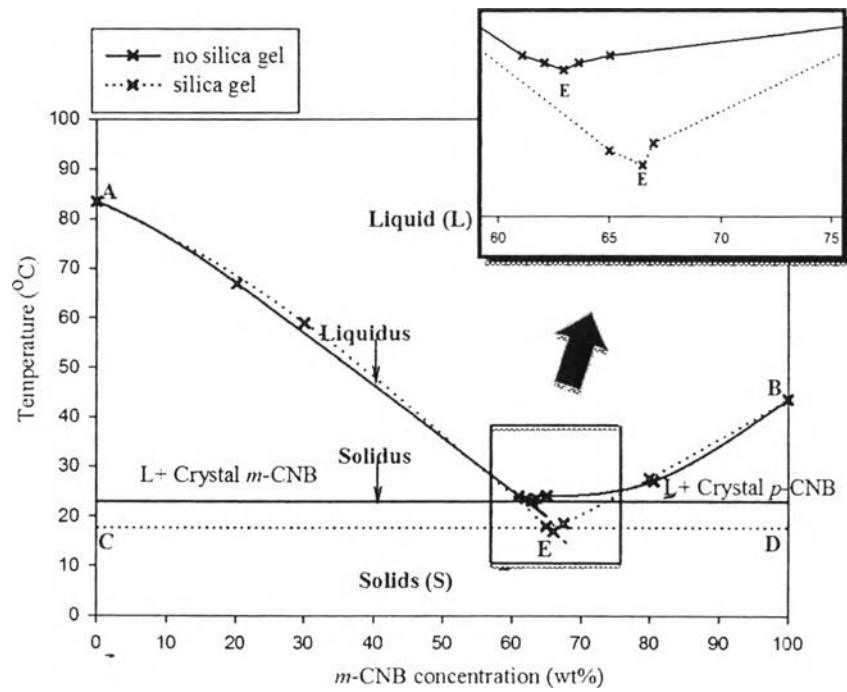* The number in the parenthesis refers to number of run.

Figure 4.6 Liquid solid phase diagram of *m*- and *p*-CNB without and with the silica gel.
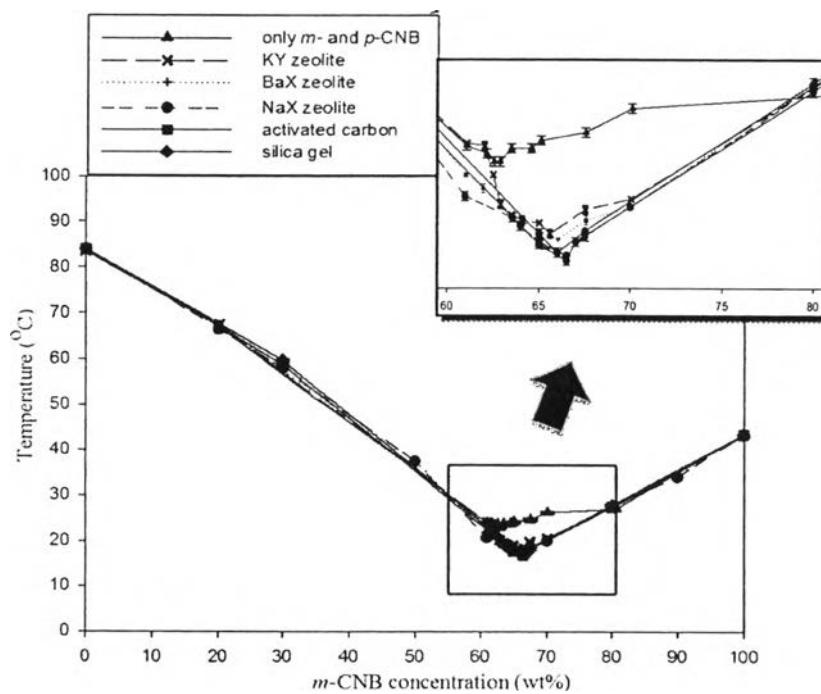

Figure 4.7 Effects of KY zeolite, BaX zeolite, NaX zeolite, activated carbon, and silica gel on the Binary phase diagram of *m*- and *p*-CNB.

Comparison the effects of the KY zeolite, BaX zeolite, NaX zeolite, activated carbon, and silica gel on the binary phase diagram of *m*- and *p*-CNB is shown in Figure 4.7. Adding the KY zeolite into the CNB mixture results in the decrease in the crystallization temperature and increase in the eutectic composition on the binary phase diagram. The same behavior can also be observed when the KY zeolite is changed to other zeolites, BaX and NaX zeolites, or amorphous materials, activated carbon and silica gel. Results from this experiment show that regardless of *m*-CNB selectivity or even type of solid material in the CNB mixture, the presence of a solid material has more or less the same behavior. Effects of a solid material may only play a role as impurity rather than having any role on the adsorption.

4.3 Roles of Zeolites and Amorphous Materials on the Crystallization and Composition of *m*- and *p*-CNB

A results show that the addition of the zeolites or amorphous materials into the mixture CNB results in the change in the phase diagram of *m*-and *p*-CNB. Crystallization temperature decreases, and the eutectic composition increases. It may be explained that the added materials may act as impurity in the form of seeding and change the boundary between the stable zone and metastable zone. Explanation of this behavior can be made from Figure 4.8. The metastable zone width is explained by the solubility - supersolubility diagram, as shown in Figure 4.9 for interfacial tension associates with the overall free energy change under heterogeneous conditions $\Delta G'_{crit}$ and the overall free energy change under homogeneous nucleation $\Delta \bar{G}_{crit}$. The relationship between supersaturation and spontaneous crystallization led to a diagrammatic representation of the metastable zone on solubility – supersolubility diagram, as shown in Figure 4.8. The lower continuous solubility curve can be located with precision. The upper broken supersolubility curve, which represents temperatures and concentrations, at which uncontrolled spontaneous crystallization occurs, is not as well defined as that of the solubility curve. Its position in the diagram is considerably affected by, amongst other things, the rate at which supersaturation is generated, the intensity of agitation, the presence of trace

impurities and the thermal history of the solution. The diagram is divided into three zone (Mullin, 2001):

1. The stable (unsaturated) zone, where crystallization is impossible.

2. The metastable (supersaturated) zone, between the solubility and supersolubility curve, where spontaneous crystallization is impossible. However, if a crystal seed were placed in such a metastable solution, growth would occur on it.

3. The unstable or labile (supersaturated) zone, where spontaneous crystallization is possible, but not inevitable.
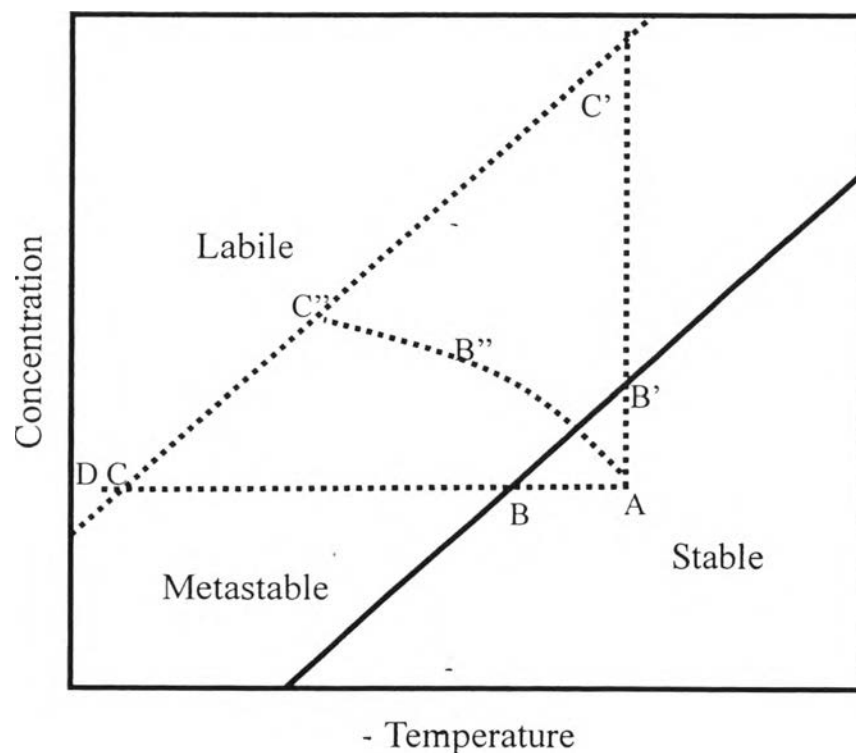
Figure 4.8 Solubility - supersolubility diagram (Mullin, 2001).

If a solution represented by point A in Figure 4.8 is cooled (line ABC), spontaneous crystallization cannot occur until conditions represen by point C are reached. At this point, crystallization may be spontaneous or it may be induced by seeding, agitation or mechanical shock. Further cooling to some point D may be necessary before crystallization can be induced. The position in the diagram is

considerably effected by the presence of trace impurities so that the presence of adsorbent in the CNB mixture may change the position in the diagram as well.

The maximum allowable supersaturation, Δc_{max}, may be expressed in terms of the maximum allowable undercooling, $\Delta \theta_{max}$:

$$\Delta c_{max} = \left(\frac{dc^{*}}{d\theta} \right) \Delta \theta_{max} \qquad (4.1)$$

As the presence of a suitable foreign body or 'sympathic' surface can induce nucleation at degree of supercooling lower than those required for spontaneous nucleation (Mullin, 2001). This sentence is consistent with crystallization temperature in the presence of the zeolites or amorphous materials, which is lower than in the absence of the solid materials.

When the degree of supercooling decreases, $\Delta \theta_{max}$ and Δc_{max} increase according to the relationship between $\Delta \theta_{max}$ and Δc_{max} in Equation (4.1). Increasing $\Delta \theta_{max}$ and Δc_{max} results in a broader metastable zone width.

The overall free energy change associated with the formation of a critical nucleus under heterogeneous conditions, $\Delta G'_{crit}$, must be less than the corresponding free energy change, ΔG_{crit}, associated with homogeneous nucleation, i.e. (Mullin, 2001).

$$\Delta G'_{crit} = \phi \Delta G_{crit} \qquad (4.2)$$

where the factor ϕ is less than unity.

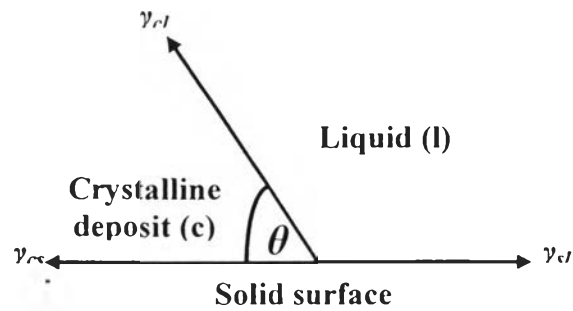**Figure 4.9** Interfacial tension at the boundaries between three phases (two solids, one liquid) (Mullin, 2001).

The interfacial tension, γ, is one of the important factors controlling the nucleation process. Figure 4.9 shows an interfacial energy diagram for three phases in contact; in this case, however, the three phases are two solids and a liquid. The three interfacial tensions are denoted by γ_{cl} (between the solid crystalline phase, c, and the liquid l), γ_{sl} (between another foreign solid surface, s, and the liquid) and γ_{cs} (between the solid crystalline phase and foreign solid surface) (Mullin, 2001). Resolving these forces in a horizontal direction

$$\gamma_{sl} = \gamma_{cs} + \gamma_{cl} \cos\theta \qquad (4.3)$$

or

$$\cos\theta = \frac{\gamma_{sl} - \gamma_{cs}}{\gamma_{cl}} \qquad (4.4)$$

The angle, θ, of contact between the crystalline deposit and foreign solid surface, corresponds to the angle of wetting in liquid-solid system (Mullin, 2001).

The factor ϕ in Equation (4.2) can be express as

$$\varphi = \frac{(2 + \cos\theta)(1 - \cos\theta)^2}{4} \qquad (4.5)$$

Thus, when $\theta=180°$, $\cos\theta=-1$ and $\phi=1$, Equation (4.2) becomes

$$\Delta G'_{crit} = \Delta G_{crit} \qquad (4.6)$$

When θ lines between 0 and 180°, $\phi < 1$; therefore,

$$\Delta G'_{crit} < \Delta G_{crit} \qquad (4.7)$$

When $\theta = 0$, $\phi = 0$, and

$$\Delta G'_{crit} = 0 \qquad (4.8)$$

This is illustrated in Figure (4.10), which shows a foreign particle in a supersaturated solution (Mersmann, 2001).

For the cases of complete non-affinity between the crystalline solid and the foreign solid surface (corresponding to that of complete non - wetting in liquid - solid system), $\theta=180°$, and Equation (4.6) applies, i.e. the overall free energy of nucleation is the same as that required for homogeneous or spontaneous nucleation.
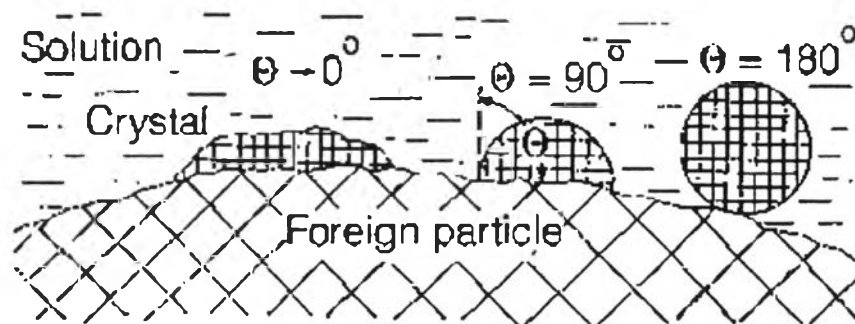

Figure 4.10 Nucleation on a foreign particle for different wetting angles (Mersmann, 2001).

For the case of partial affinity (cf. the partial wetting of a solid with a liquid), $0<\theta<180°$, and Equation (4.7) applies, which indicates that nucleation is easier to achieve because the overall excess free energy required is less than that for

homogeneous nucleation. For the case of complete affinity (cf. complete wetting) $\theta = 0$, and the free energy of nucleation of zero. This case corresponds to the seeding of a supersaturation solution with crystals of the required crystalline product, i.e. no nuclei have to be formed in the solution (Mullin, 2001).

The presence of the zeolites or amorphous materials may be in the case of the partial wetting of a solid with a liquid, which is described by Equation (4.7), and ΔG_{crit} is related to $(\Delta T)^{-2}$, as indicated in Equation (4.9).

$$\Delta G_{crit} \; \alpha \; (\Delta T)^{-2} \tag{4.9}$$

where $\Delta T = T^* - T$ is the supercooling, T^* is the solid-liquid equilibrium temperature, and T is degree of supersaturation (Mullin, 2001).

From Equations (4.2), (4.7) and (4.9), the value of $\Delta G'_{crit}$ will be less than ΔG_{crit} when the value of ΔT is high, meaning that the value of T or degree of supersaturation must be low. This relates to "The presence of a suitable foreign body or 'sympathic' surface can induce nucleation at degree of supercooling lower than those required for spontaneous nucleation (Mullin, 2001)." The metastable zone width may become broader. Thus, the crystallization temperature of the feed with the zeolites or amorphous materials decreases from the crystallization temperature of the feed without. The presence of the zeolites or amorphous materials may change the properties of the solution structure. The binary phase diagram of m- and p-CNB is shifted to the right hand side. That is a reason why the precipitate composition in the feed at and above the eutectic composition is shifted from being rich in m-CNB to p-CNB.